Progress Report on "Penn State Activities in the NASA GSFC Transmissive Microshutter Array Technology Development Program" (NASA NAG5-10617, 04/01/01-03/31/02)

Jian Ge, Dept. of Astronomy & Astrophysics, Penn State University
Tel: 814-863-9553, Fax: 814-863-3399, Email: jian@astro.psu.edu

1. Project Description

This is a one year contract starting on April 1, 2001 to design the Rapid Infrared and Visible Multiple Object Spectrometer (RIVMOS) and its auxiliary dispersing elements, design and fabricate silicon grisms, and reduce testing data with silicon grisms. Here I report our progress made during the funding period.

2. Research and Development (4/01/01 – 03/31/02)

2.1 Design of RIVMOS

A wide field (6×6 arcmin^2) Rapid Infrared-Visible Multi-Object Spectrometer (RIVMOS) has been designed as part of the Next Generation Space Telescope (NGST) development and new technology demonstration. The primary goal is to demonstrate that the microshutter arrays, currently being designed for the NGST Near Infrared Spectrometer (NIRSpec) as programmable 2D selection masks, can achieve the optical performance required for faint object imaging and spectroscopy. The optical design includes both reflective and refractive optics. The required

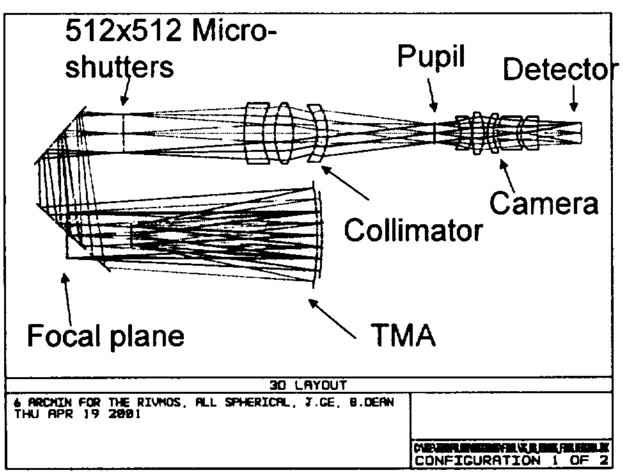

RMS spot diagram at 1.5 μm

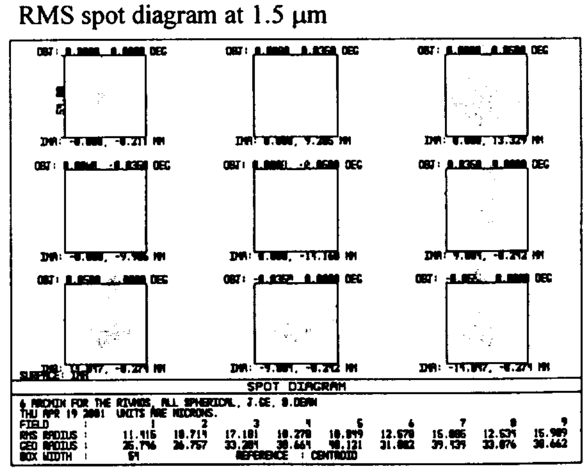

Figure 1. (Left) the layout of the optical design of RIVMOS imaging mode, it a three-mirror anastigmat (TMA), collimator, camera and detector. (Right) RMS spot diagrams within the 6×6 acrmin^2 FOV. The square box represents 2×2 InSb detector pixels (or 54×54 μm^2).

optical performance is achieved for both multi-object spectroscopy and camera imaging over the entire field-of-view. The optical design consists of six optical subsystems including (1) an image relay consisting of a three-mirror anastigmat (TMA), (2) the microshutter assembly, (3) a triplet collimating optic, (4) a grism/filter assembly, (5) a pupil imaging optic, and (6) a five element telecentric camera design.

The all-spherical optical design reduces construction costs and facilitates fabrication of the optical assembly while maintaining an encircled energy of 2 pixels within the FOV for wavelengths between 0.6 and 5.0 microns. The 512×512 microshutter array is located at the cold focal plane formed by the TMA, which provides the required spatial sampling on the

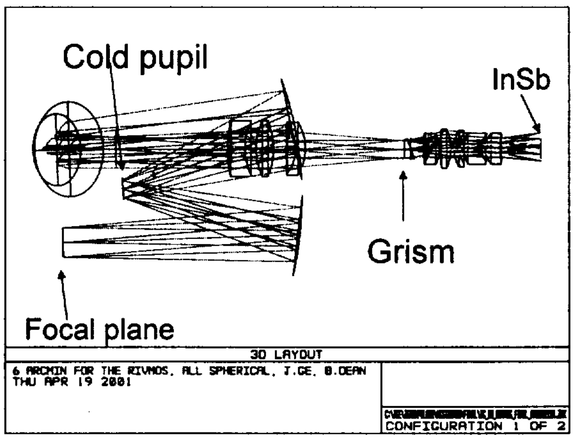

RMS spot diagram at 1.8 μm, middle of MOS spectra

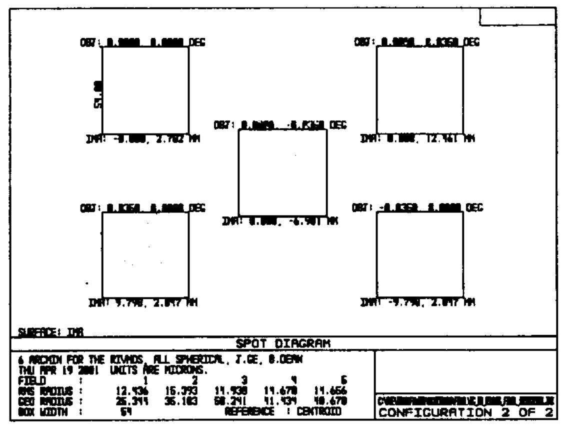

Figure 2. (Left) the layout of the optical design of RIVMOS spectroscopy mode. The optics are the same except a grism is inserted at the pupil location for dispersing the incoming beam. (Right) RMS spot diagrams for dispersed light within the detector. The square box represents 2×2 InSb detector pixels (or 54×54 μm^2).

microshutter array. The TMA relay also forms a cold pupil on its secondary where a cold pupil mask is located to reject extraneous thermal emissions from the telescope structure, such as the central obscuration. This design of the TMA is a novel variation on the classical Offner relay. The vertices are constrained in a fashion that gives diffraction-limited imagery at the micro-shutter, while using only spherical surfaces. Not only does this eliminate the need for aspherical surfaces, but also induced astigmatism is corrected which ultimately results in a simpler camera design.

Figure 1 shows the optical layout of the imaging mode in RIVMOS and its spot diagrams within the 6 arcmin FOV. More than 80% encircled energy is within 2x2 pixels. The spectroscopy will be conducted by inserting a grism on a filter wheel at the last pupil location. Figure 2 shows the optical layout of the spectroscopy mode with R = 1000 and its spot diagrams within the 1k×1k detector. More than 80% encircled energy is within 2x2 pixels. Therefore, our design for imaging and spectroscopy meets the requirement for demonstrating the capability of the micro-shutter array for scientific observations.

2.2 Development of New Processes for Making High Quality Silicon Gratings:

(a). TMAH +AP process

Late in 2001, we developed a new etching process with Tetramethyl ammonium hydroxide (TMAH), ammonium persulfate (AP) and a thin silicon dioxide mask (~ 100 nm thickness) and post-processing process, which helps us to significantly reduce grating surface roughness. By the end of the year, we were able to reach ~ 15 nm rms roughness for the silicon wafer gratings with

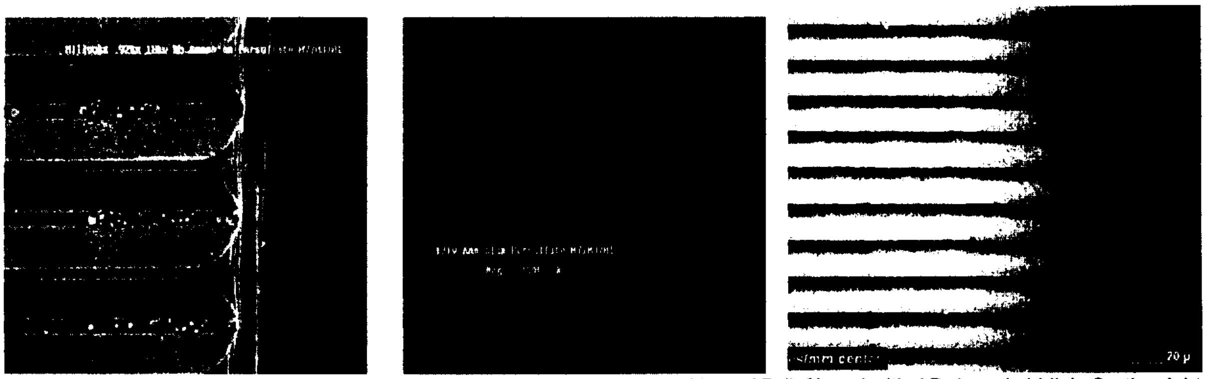

Figure 3. The etched silicon wafer gratings with the TMAH process and without AP (left) and with AP dose (middle). On the right, a fused-silica transmission grating with 10 μm grooves, commercially made by Richardson grating company, is shown for comparison. Irregularity and surface roughness can be clearly seen in this commercial grating.

10×10 mm^2 etched area and 66 μm grooves. This roughness is a factor of 2 times lower than that in November 2001. Scanning electron micrograph (SEM) pictures of etched gratings with and without AP processes are shown in Figure 3. The grating with the AP process has much smoother grating facet surfaces and less defects. **The grating with the AP process represents our first significant improvement in grating surface quality with the NASA support.** For a direct comparison, we have also shown a commercially made grating surface under a 100x

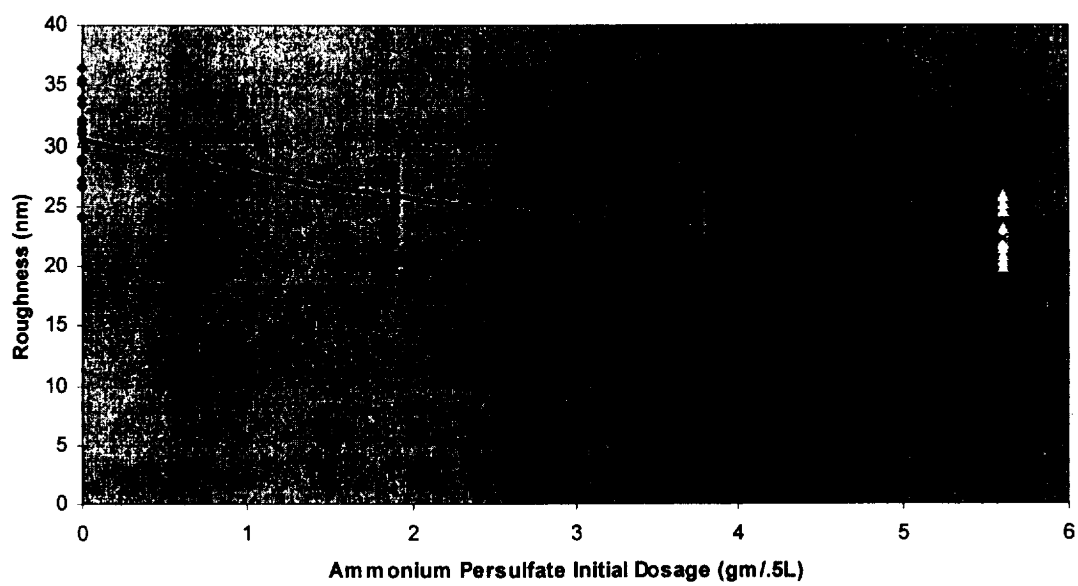

Figure 4. Progression of reduced roughness with increased amounts of ammonium persulfate.

optical microscope. Visually, there are many uneven grooves which are caused by the replication process and also transfer of defects in the master grating made through mechanical ruling, the traditional grating fabrication technique. Our grating made by the TMAH and AP chemical etching process shows very organized groove structures and also smoother grating surfaces.

Quantitative measurements of these etched gratings with and without AP processes shown in Figure 4 indicate roughness reduction depends on the dose of the AP in the TMAH etchant. The total improvement in surface roughness can reach ~ 32%, which is being reported in a paper (McDavitt, Ge et al. 2002 in preparation). In addition, as shown in Figure 3, defects on the grating surfaces are significantly reduced with the AP process. Our examination under a 10x optical microscope shows that visible defects with typical dimension of ~ a few microns or larger have been reduced to less than 1 per cm^2 from originally more than 100 per cm^2 a year ago.

(b). Post-processing

Further improvement in surface roughness has also been observed in our post-processing. This process involves application of a thin oxide layer, usually ~ 20 nm to finished grating surfaces and etching away of the oxide layer with buffled HF (BHF). This takes advantage of different oxide growth rate at different location of an uneven silicon surface. As illustrated in Figure 5, the rms surface roughness has been further reduced by ~ 25% after a single post-processing run (Bernecker, Ge et al. 2002 in preparation). The lowest rms toughness we achieved with a combination of the AP and the post processing is about 15 nm. We have also found that the average surface roughness increased slightly after two runs. In addition, grating surface becomes much rougher after three post-processing runs. Upon investigation, it was discovered that pits had formed in the three run gratings. The pits on the Czechralski (CZ) wafers three run samples ranged in size from 0.2-0.3μm and 2.5-3μm. Those on the float zone (FZ) wafers three run samples ranged in size from 0.5-1μm. Our conclusion is the single run of post-processing run gives the smoothest grating surface.

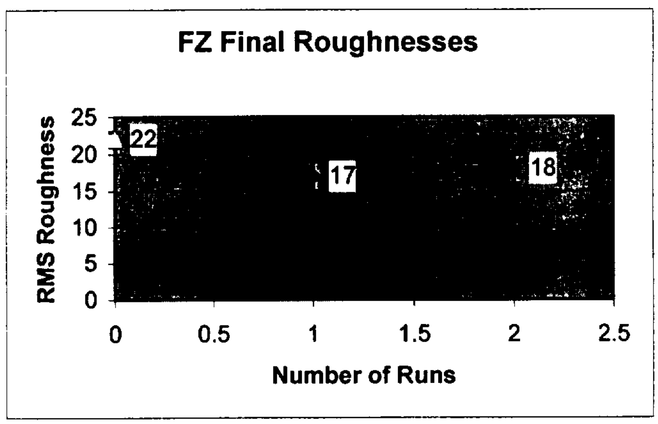

Figure 5. Surface roughness without (rms ~ 22 nm) and with (rms ~17 nm) our newly developed post-processing.

2.3 Optical Performance of the Etched Silicon Gratings

(a). Precise surface roughness measurements by the Atomic Force Microscope (AFM)

The RMS surface roughness reported values above were from the measurements with a profilometer at the Penn State Nanofab. Since the stylus of the profilometer has a resolution of ~ 10 μm, the measurements is a convolution of the stylus sensitivity and grating surface roughness. These results can only represent estimated surface quality over a large scale (typically a few hundreds of microns). A much better way to evaluate the surface roughness, especially on the scale of ~ μm is through an atomic force microscope (AFM). Figure 6 shows comparison of AFM surface roughness among etched gratings over a period of 8 months. These measurements were conducted at the Penn State Material Research Institute. It is very clear that the grating surface gets much smoother in June 2002. In November 2001, the typical RMS surface roughness for the best etched silicon gratings with the TMAH and AP process over ~ 1 μm scale is 9 nm. In March 2002, the RMS surface roughness for the best etched gratings is down to 3 nm. In June 2002, the rms roughness is reduced to 0.9 nm. **The surface roughness for these gratings is lower than that for the HST mirror, 12 nm.**

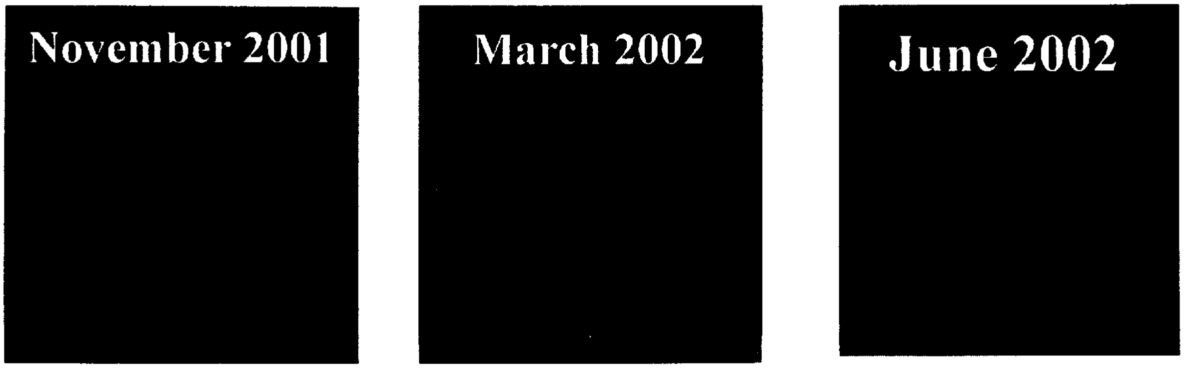

Figure 6. Atomic Force Microscope scanning of the best etched silicon gratings in November 2001, March 2002 and June 2002. The RMS surface roughness over 2 μm in randomly chosen grating surfaces are 9 nm, 3 nm and 0.9 nm from the right to the left, respectively.

(b). Integrated scattered light measurements

An etched grating with ~ 15 nm rms roughness has been evaluated with our optical spectrograph. The total measured integrated scatter at 0.633 μm is less than 1% scatter as shown in Figure 7. This level of scatter is already a factor of three times better than that of a commercial 23.2 l/mm echelle grating measured Kuzmenko & Ciarlo in 1998. It is also a factor of ~ 10 times better than previous results by other groups (Kuzmenko et al. 1998; Keller et al. 2000).

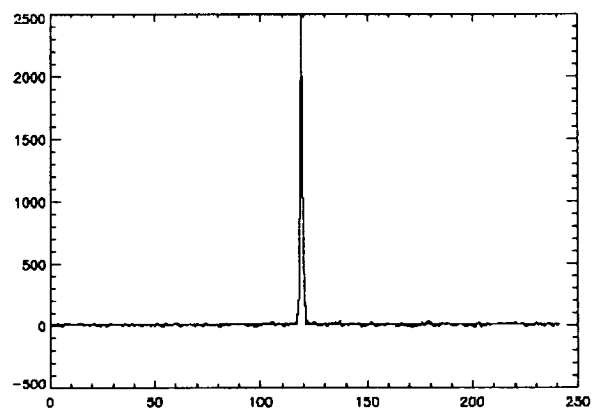

Figure 7. Cross-section of a HeNe laser at 0.6328 μm, indicating <1% integrated scattered light for the TMAH etched grating.

(c). Wavefront quality of etched gratings

Wavefront quality of the etched gratings has been evaluated by a Zygo interferometer at Lawrence Livermore National Lab through collaborating with Dr. P. Kuzmenko. Figure 8 shows the wavefront over 10×10 mm^2 etched grating area at 0.6328 μm in reflection. The RMS wavefront distortion is 0.035 waves, indicating diffraction-limited performance once the grating is operated in both immersed reflection and transmission. The high wavefront quality was achieved through using very thin oxide grating mask layer with typical thickness of 1000 Å. Our previous study shows that sharp mask pattern is the critical step for maintaining wavefront quality (Ge et al. 2002). This is why etched gratings with a plasma etching have better quality than those with wet etching. However, it is challenging to make masks on thick silicon substrates in the plasma chamber. Our thin mask layer made through a wet processing can maintain the grating pattern as sharp as those plasma-etched grating mask, resulting in high wavefront quality. Maintaining high wavefront quality is critical for achieving the highest dispersion power provided by silicon immersion gratings.

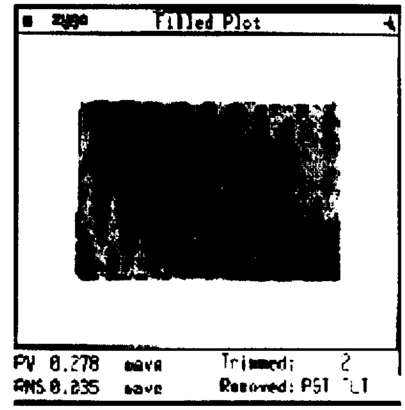

Figure 8. Wavefront map of a silicon grating with 10×10 mm^2 etched area at 0.6328 μm measured by a Zygo interferometer. The grating was made with the new TMAH+AP etching.

2.4 Silicon Grisms Made through New Processes

The new etching technique, TMAH + AP process, has been applied in fabricating new generation silicon grisms. Figure 9 shows etched gratings on two silicon substrates with 100 mm in diameter and 20 mm thickness. One has 16 gratings. Each grating has 10×10 mm^2 etched area, a 54.7 deg blaze angle and 66 μm period grating grooves. The other has 4 gratings. Each has 25×25 mm^2 etched area, a 54.7 blaze angle, and 13 μm grating grooves. The surface roughness of one of the gratings with 66 μm grooves has been measured by the profilometer and shows ~ 15 nm rms roughness. These gratings have been cut and polished by SPEC Precision Optics Inc. in Tennessee. Figure 10 shows 4 finished grisms installed in mechnical mounts. The three smaller grisms are for testing and observing with our Penn State near IR Imager and Spectrograph (PIRIS). The larger one is for testing and observing at the Arizona Imager and Echelle Spectrograph (ARIES) at the MMT 6.5-m telescope. Recent lab testing shows that the integrated light levels from silicon grisms has the total integrated scattered light level of about 1% in the entire near-IR, 10 times better than our prototype made at LLNL in 2000.

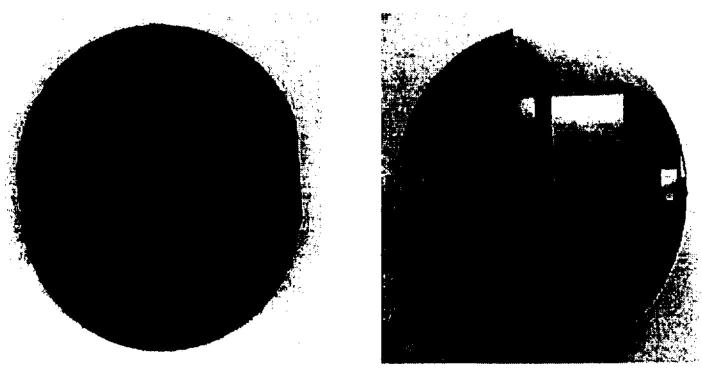

Figure 9. Etched gratings on thick silicon substrates with the newly developed TMAH and AP etching process at Penn State. The gratings on the left have 10×10 mm^2 etched area and 66 μm grating period. The gratings on the right have 25×25 mm^2 etched area and 13 μm grating period.

2.5 Grating Performance Modeling

In addition to developing new grating fabrication processes, we have also conducted grating efficiency modeling using commercially available G-solver software in 2002. Figure 11 shows design of a silicon grism with 7.3 μm grooves and 22 deg

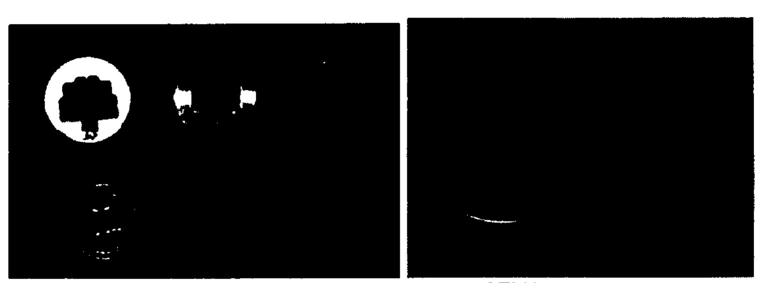

Figure 10. New generation of silicon grisms made of TMAH plus AP processes are mounted in holders and ready for observing with PIRIS (the left three, with etched areas of ~ 10x10 mm^2) and ARIES (the right one, with etched area of 15x15 mm^2).

blaze in the J, H, K, L and M bands for RIVMOS. The grating efficiency is also shown in the Figure. The grism is operated in the first order at the M band, the 2nd order for the L band, the 3rd

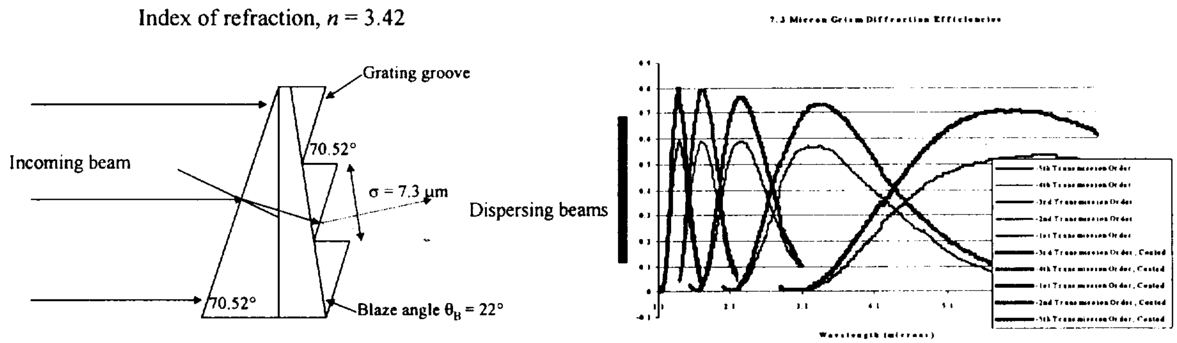

Figure 11. (Left) Design of a silicon grism with 7.3 μm groove and 22 deg blaze angle for RIVMOS. (Right) Modeling of the silicon grism in the J, H, K, L and M bands (Ge et al. 2002).

order fot the K band, the 4th order for the H band and 5th order for the J band. This modeling has assumed that no scattered light loss. Without anti-reflection coating, the peak efficiency is about 60% for all these bands. With a single layer silicon nitride coating, the peak efficiency can reach 80%, which is beyond any of commercially available low resolution grisms (Rayner 1998; about 45% efficiency for the KRS-5 grisms in the Gemini NIRI camera, Simons 2001, private communications). This grism will provide R = 2000 in 1.2 – 5.5 μm with RIVMOS (Ge et al. 2002). We are about to purchase thick silicon substrates and make these grisms in 2003.

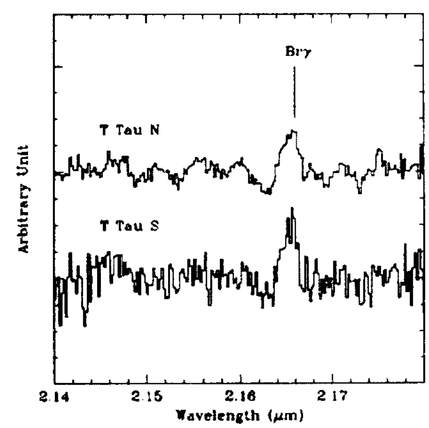

Figure 12. Reduced spectra of T Tau N and S components, showing Brγ emission lines.

2.6 Silicon Grism Spectral Data Reduction

The cross-dispersed echelle spectra taken with our second-generation silicon grisms at the Lick Observatory were reduced and analyzed by my team in the Spring 2002. Data analysis shows that Brγ emission lines are associated with both T Tauri N and S components (Figure 12), similar to what have been found by the Keck AO IR spectroscopy (Duchene et al. 2002; Ge et al. 2002). The spectrum of BD+65 1638 shows an enormous broad Brγ absorption with a FWHM of 550 ± 50 km/s (~ 90% of stellar brake-up velocity) (Figure 13), indicating this star is perhaps undergoing an early phase of slowing the stellar rotation down to become a normal Be star (Ge et al. 2002; Chakraborty et al. 2002). These observations demonstrate the scientific capabilities of silicon grisms. Two scientific papers are being written to report the new scientific discoveries with the silicon grisms.

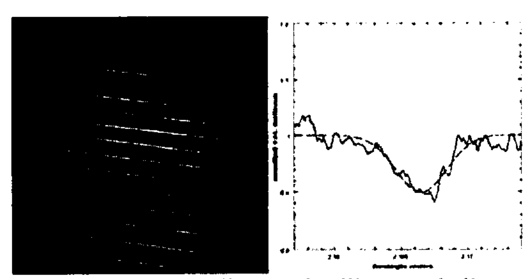

Figure 13. Cross-dispersed silicon echelle grism spectrum of BD 65+1638, a Be star, in the K band. It completely covers 2.0-2.4 μm. The cross-disperser is a low resolution CaF_2 grism.

2.7 Technical and Scientific Publications

The following list is the papers or presentation published in the scientific journals and proceedings which are related to this project:

Published:

- Ge, J., McDavitt, D., Bernecker, J., Ciarlo, D., & Kuzmenko, P. 2001,"Development of Silicon Grisms and Immersion Gratings fir High-resolution IR spectroscopy", Proc. SPIE, 4485, 393
- Debes, J.H., Ge, J., & Chakraborty, A., 2002, "First High Contrast Imaging Using a Gaussian Aperture Pupil Mask," ApJ, 572, L165
- Chakraborty, A., Ge, J., & Debes, J.H., 2002, "Nature of Faint Companions to G-type Stars Using Adaptive Optics," AJ, 124, 1127
- McDavitt, D., Ge, J., Bernecker, J., & Miller, S., 2001, "Improved Results in the Development of Large Silicon Grisms using New Techniques," *BAAS*, 199, 10207
- Ge, J., et al. 2001, "Extra-solar Planet Studies with New Instrument Technology at Penn State," *BAAS*, 199, 3304

In press:

- Ge, J., et al. 2002, "Compact High-resolution 3D Imaging Spectrometer for Discovering Oases on Mars," Proc. SPIE, 4859, in press
- Ge, J., et al. 2002, "Breakthroughs in silicon grism and immersion grating technology at Penn State", Proc. SPIE, 4841, in press
- Ge et al. 2002, "New generation IR instrument components ready for NGST", Proc. SPIE 4850, in press
- Ge et al. 2002, "Silicon anamorphic gratings for IR high resolution spectroscopy with future giant telescopes", Proc. 4840, in press

Drafts to be submitted:

- Ge, J., et al. 2002, "First high resolution IR spectroscopy with a silicon grism," to be submitted to ApJ Letters
- Ge, J., et al. 2002, "Silicon grisms for high resolution IR spectroscopy," to be submitted to PASP
- Bernecker, J., Ge, J., Miller, S., & McDavitt, D., 2002, "A Post-processing Technique for Improving Si {111} Surface Roughness on Silicon Gratings," to be submitted to Sensor and Actuator
- McDavitt, D., Ge, J., Miller, S., & Bernecker, J., 2002, "Improved Etching of Silicon Gratings using Ammonium Persulfate", to be submitted to J. Micromechan. Microeng.
- Chakraborty, A., & Ge, J., 2002, "Birth of a Be Star, BD+65 1638: New Spectroscopic Observations Using Adaptive Optics and Silicon Grism," to be submitted to ApJ